

See discussions, stats, and author profiles for this publication at: <https://www.researchgate.net/publication/43078695>

# The Major Protein of Bovine Seminal Plasma, PDC-109, Is a Molecular Chaperone

ARTICLE *in* BIOCHEMISTRY · APRIL 2010

Impact Factor: 3.02 · DOI: 10.1021/bi100051d · Source: PubMed

---

CITATIONS

23

---

READS

47

## 2 AUTHORS:



Rajeshwer Sankhala

Thomas Jefferson University

15 PUBLICATIONS 76 CITATIONS

SEE PROFILE



Musti J. Swamy

University of Hyderabad

139 PUBLICATIONS 2,102 CITATIONS

SEE PROFILE

# The Major Protein of Bovine Seminal Plasma, PDC-109, Is a Molecular Chaperone<sup>†</sup>

Rajeshwer Singh Sankhala and Musti J. Swamy\*

*School of Chemistry, University of Hyderabad, Hyderabad-500046, India*

*Received January 13, 2010; Revised Manuscript Received March 22, 2010*

**ABSTRACT:** The major protein of bovine seminal plasma, PDC-109, binds to choline phospholipids on the sperm plasma membrane and induces the efflux of cholesterol and choline phospholipids, which is an important step in sperm capacitation. The high abundance, polydisperse nature and reversibility of thermal unfolding of PDC-109 suggest significant similarities to chaperone-like proteins such as spectrin,  $\alpha$ -crystallin, and  $\alpha$ -synuclein. In the present study, biochemical and biophysical approaches were employed to investigate the chaperone-like activity of PDC-109. The effect of various stress factors such as high temperature, chemical denaturant (urea), and acidic pH on target proteins such as lactate dehydrogenase, alcohol dehydrogenase, and insulin were studied in both the presence and absence of PDC-109. The results obtained indicate that PDC-109 exhibits chaperone-like activity, as evidenced by its ability to suppress the nonspecific aggregation of target proteins and direct them into productive folding. Atomic force microscopic studies demonstrate that PDC-109 effectively prevents the fibrillation of insulin, which is of considerable significance since amyloidogenesis has been reported to be a serious problem during sperm maturation in certain species. Binding of phosphorylcholine or high ionic strength in the medium inhibited the chaperone-like activity of PDC-109, suggesting that most likely the aggregation state of the protein is important for the chaperone function. These observations show that PDC-109 functions as a molecular chaperone *in vitro*, suggesting that it may assist the proper folding of proteins involved in the bovine sperm capacitation pathway. To the best of our knowledge, this is the first study reporting chaperone-like activity of a seminal plasma protein.

In mammals, seminal plasma serves as a carrier for the spermatozoa in their journey from the male testes to the female uterus, where sperm–egg fusion takes place, resulting in fertilization. The seminal plasma is a complex fluid and contains organic as well as inorganic molecules of low and high molecular weight. While the low molecular weight fraction contains a wide variety of chemical species, proteins are the only high molecular weight constituents found in seminal plasma; other biopolymers such as polysaccharides and nucleic acids are not present in it (1).

Among the various mammalian species, proteins from the bovine seminal plasma have been investigated extensively. In particular, the major protein of the bovine seminal plasma, PDC-109, has been studied in great detail (2–17). It is a protein with 109 amino acid residues, made up of two tandemly repeating fibronectin type II (FnII)<sup>1</sup> domains (2, 3). Each of these domains

contains one choline-binding site (4). PDC-109 exists as a polydisperse aggregate in solution, and its thermal unfolding is partially reversible (5). Single-crystal X-ray diffraction studies on PDC-109 complexed with phosphorylcholine (PrC) show that both the choline-binding sites are on the same face of the protein (6). Upon ejaculation, around 9.5 million PDC-109 molecules bind to each spermatozoon (7). This interaction is mediated by the binding of PDC-109 to choline phospholipids such as phosphatidylcholine (PC) and sphingomyelin, present on the outer leaflet of the sperm plasma membrane (8). Biophysical studies on the interaction of PDC-109 with different lipid membranes have shown that although PDC-109 recognizes choline phospholipids with greater specificity, it also recognizes other phospholipids such as phosphatidylglycerol and phosphatidylserine, albeit with considerably lower specificity (9–12). Binding of PDC-109 leads to the extraction of lipids and cholesterol from sperm plasma membrane, a process referred to as cholesterol efflux, which appears to be a critical step in sperm capacitation (16, 17).

Some of the characteristics exhibited by PDC-109 such as polydispersity, high abundance, and reversibility of thermal unfolding are quite similar to those displayed by well-characterized stress proteins with chaperone-like activity such as spectrin and  $\alpha$ -crystallin. This prompted us to investigate whether PDC-109 can function as a molecular chaperone. Stress proteins are part of the antistress mechanism that all cells possess to deal with stress (18). Some stress proteins are molecular chaperones, which constitute the cellular chaperoning system. These systems play a central role in cell physiology both under normal and stress conditions by assisting in the folding of newly synthesized

<sup>†</sup>This work was supported by a research grant from the Department of Science and Technology (India) to M.J.S. R.S.S. is a Senior Research Fellow of the CSIR (India). We acknowledge the University Grants Commission (India) for their support through the UPE and CAS programs to the University of Hyderabad and School of Chemistry, respectively.

\*To whom corresponding should be addressed. Tel: +91-40-2313-4807. Fax: +91-40-2301-2460. E-mail: mjssc@uohyd.ernet.in, mjswamy1@gmail.com.

Abbreviations: ADH, alcohol dehydrogenase; AFM, atomic force microscopy; CD, circular dichroism; CDNB, 1-chloro-2, 4-dinitrobenzene; FFT, fast Fourier transform; FnII, fibronectin type II; G6P, glucose 6-phosphate; G6PD, glucose-6-phosphate dehydrogenase; GSH, glutathione; GST, glutathione S-transferase; LDH, lactate dehydrogenase; MOPS, 3-(*N*-morpholino)propanesulfonic acid; NADP, nicotinamide adenine dinucleotide phosphate; PC, phosphatidylcholine; PrC, phosphorylcholine; TBS-I, 50 mM Tris buffer containing 0.15 M NaCl and 5 mM EDTA, pH 7.4; ThT, thioflavin T.

polypeptides. Molecular chaperones also assist in the refolding of proteins that are partially denatured due to stress and in the dissolution of pathological protein aggregates etc. (19–22). The first step in the protective action of a molecular chaperone is its interaction with denatured or unfolded proteins to provide a suitable environment to facilitate their normal folding or prevent the formation of large protein aggregates (23–26).

In the present study, biochemical assays aimed at investigating the chaperone-like activity of PDC-109 have been performed, which demonstrated that this protein is able to effectively prevent the unfolding and aggregation of target proteins such as insulin, lactate dehydrogenase (LDH), alcohol dehydrogenase (ADH), and  $\beta_L$ -crystallin. It has been also shown that PDC-109 protects enzymes such as glucose-6-phosphate dehydrogenase (G6PD) and glutathione *S*-transferase (GST) against thermal and chaotrope-induced inactivation, respectively. The aggregation and chaperone-induced disaggregation processes have been characterized in detail by atomic force microscopy (AFM) and image processing of the AFM data. Refolding of target proteins was arrested by PDC-109 in a concentration-dependent manner, similar to some other heat-shock proteins such as spectrin and Hsp90 (27, 28). Binding of PrC and choline to PDC-109 as well as the presence of a high concentration of sodium chloride and EDTA in the medium resulted in an inhibition of the chaperone-like activity of the protein, suggesting that the aggregation state of the protein is likely to be important for the chaperone-like activity of PDC-109. The results obtained clearly demonstrate that PDC-109 exhibits chaperone-like activity which is likely to be physiologically significant.

## MATERIALS AND METHODS

**Materials.** Choline chloride, phosphorylcholine chloride, insulin, G6PD (from *Leuconostoc mesenteroides*), glucose 6-phosphate (G6P), GST, thioflavin T (ThT), 1-chloro-2,4-dinitrobenzene (CDNB), and MOPS were from Sigma (St. Louis, MO). Sephadex G-50 (superfine) and DEAE-Sephadex A-25 were obtained from Pharmacia (Uppsala, Sweden). LDH (from rabbit muscle), ADH (from baker's yeast), nicotinamide adenine dinucleotide phosphate (NADP), Tris base, glutathione, and other chemicals were purchased from local suppliers and were of the highest purity available.  $\beta_L$ -Crystallin from bovine eye lens was a kind gift from Dr. G. B. Reddy (National Institute of Nutrition, Hyderabad, India). PDC-109 was purified as described earlier (9). The purified protein was dialyzed extensively against 50 mM Tris buffer, 0.15 M NaCl, and 5 mM EDTA, pH 7.4 (TBS-I), and stored at 4 °C.

**PDC-109-Assisted Reactivation of Heat-Denatured G6PD.** G6PD activity was assayed by a spectrophotometric method (29). In this assay G6P is oxidized to 6-phospho-D-gluconate by G6PD with simultaneous reduction of NADP to NADPH. The assay medium contained G6PD (0.25  $\mu$ M), NADP (0.1 mM), G6P (5 mM), and 12 mM each of  $MgCl_2$  and KCl. The reaction was initiated by the addition of NADP, and increase in absorbance at 340 nm due to the reduction of NADP was monitored using a Cary 100 UV/vis Bio spectrophotometer, which was also used for all other spectrophotometric measurements. To investigate the effect of PDC-109 on the thermal inactivation of the enzyme, G6PD was incubated for 30 min in the absence or presence of 0.5  $\mu$ M PDC-109 at 45 °C. Relative activity of various treated samples was normalized with respect to the activity of native G6PD.

**Aggregation-Inhibition Assay of Thermally Aggregated Enzymes.** Chaperone activity was assayed as described previously (19) by monitoring the ability of PDC-109 to prevent heat-induced aggregation of ADH at 48 °C. Aggregation was monitored by recording light scattering at 360 nm as a function of time. Concentration of ADH was 0.1 mg/mL in all the samples, and PDC-109:ADH (w/w) ratios of 1:2, 1:1.4, and 1:1 were used. The aggregation profile for the native enzyme was taken as 100%, and percent aggregation of other samples was calculated with respect to the native enzyme.

**Reactivation of Urea-Denatured GST.** Glutathione *S*-transferase activity was assayed by the CDNB-GST spectrophotometric assay (30) with a slight modification. The reaction mixture consisted of 4 mM reduced glutathione (GSH), 0.4 mM CDNB, 5  $\mu$ g of GST, and TBS-I buffer in a final volume of 1.0 mL. Reaction was initiated with the addition of GST. Unfolding of GST was performed by mixing the stock solutions of GST and urea in TBS-I buffer (pH 7.4) to give the desired concentration of protein (25  $\mu$ g/mL) and denaturant (2 M). The solution was incubated at room temperature for 1 h in the presence or absence of PDC-109 (0.5 mg/mL), followed by dialysis against TBS-I at 4 °C for 2 h to remove the denaturant. The dialyzed samples were then assayed for GST activity.

**Calorimetric Studies on PDC-109-Induced Stabilization of Target Proteins.** Thermal unfolding studies on LDH were carried out using a VP-DSC differential scanning calorimeter from MicroCal (Northampton, MA). Protein solutions in TBS-I were heated from 10 to 75 °C at a scan rate of 40 °C/h under a constant pressure of 22.9 psi. PDC-109:target protein (w/w) ratios were 1:1 and 1:1.6 for LDH. Buffer scans were subtracted from all thermograms to eliminate the contribution from buffer, and the temperature dependence of excess heat capacity was further analyzed using Origin software supplied by MicroCal.

**Inhibition of Insulin Fibrillation by PDC-109.** Insulin was dissolved in water at 0.5 mg/mL concentration, and its pH was adjusted to 1.6 with HCl. Incubation of this sample at 45 °C for 5 days yielded a turbid solution, indicating the formation of amyloid fibrils. The sample was then centrifuged at 12000g for 12 h at 15 °C in an Eppendorf 5810 R centrifuge. The supernatant was discarded, and the pellet was suspended in TBS-I. To investigate the effect of PDC-109 on insulin fibrillation, samples were prepared in the same way in the presence of 1 mg/mL PDC-109. Protein samples were diluted and used for AFM imaging as follows. A 50–80  $\mu$ L aliquot of the protein solution was carefully deposited on a freshly cleaved mica sheet (1 cm  $\times$  1 cm) and allowed to dry for 20–30 min, rinsed with HPLC grade water, dried, and transferred to the AFM stage. Imaging was performed in semicontact mode using a SOLVER PRO-M atomic force microscope (NT-MDT, Moscow, Russia), equipped with a 3.0  $\mu$ m bottom scanner. NSG10 cantilevers with Au reflective coating and a nominal spring constant of 11.8 N/m were used for the scanning. Force was kept at the lowest possible value by continuously adjusting the set point and feedback gain during imaging.

**Fluorometric Assay for Thioflavin T Binding to Insulin Fibrils.** The presence of amyloid fibrils can be detected by ThT binding assay (31). Binding of ThT to insulin fibrils, formed as described above, was studied by titrating a fixed concentration of ThT (0.1 mM) with increasing concentrations of insulin fibrils ranging from 0.43 to 6.45  $\mu$ M. Steady-state fluorescence measurements were performed on a Jobin-Yvon Spex Fluoromax-4

spectrofluorometer at 25 °C. ThT in TBS-I buffer (pH 7.4) was excited at 440 nm, and emission spectra were recorded between 450 and 550 nm. All fluorescence spectra were corrected for dilution effects.

**Inhibition of Thermal Aggregation of ADH by PDC-109.** ADH samples at a concentration of 40  $\mu\text{g/mL}$  in TBS-I were incubated in the presence and absence of 20  $\mu\text{g/mL}$  PDC-109 at 48 °C in a water bath for 30–40 min and then transferred to an ice bath. AFM samples were prepared as described above. An AFM image of native enzyme (kept at 4 °C) was used as a control. Images were analyzed using NOVA software, supplied by NT-MDT.

**(i) Average Fast Fourier Transform (FFT) Analysis.** Average FFT profiles of individual images, which indicate the periodicity of surface topography in *X* and *Y* directions, have been calculated. Fourier transformation transforms the data from time domain to frequency domain. Briefly, it shows how often which amplitudes are met on the image. FFT is used to calculate the average frequency components of a signal. Since we have used the magnitude of surface topography as a signal or FFT scaling parameter, the average FFT profile shows the average magnitude of surface topography in each frequency domain and plots it against the frequency (32). Small values of averaged FFT traces and equal distribution in all frequency regions indicate homogeneity of the samples, whereas the opposite is indicative of a less homogeneous sample or aggregated proteins.

**(ii) Roughness Analysis.** This analysis yields several statistical parameters and a distribution density histogram. The distribution density histogram indicates values of *Z*-function in the *X*-direction, whereas the *Y*-direction shows the corresponding number of points where the function value exists. Qualitatively similar results were obtained from bearing ratio analysis, which is another statistical method to analyze the AFM images (see Supporting Information and Figures S3 and S5C).

**Refolding of Denatured Enzymes.** Rabbit muscle LDH (14.28  $\mu\text{M}$ ) was incubated in 6 M GdnHCl at room temperature overnight in order to achieve complete denaturation. Refolding was initiated by a 200-fold dilution of the denatured enzyme with renaturation buffer (TBS-1, pH 7.4) in the absence and presence of different concentrations of PDC-109. Recovery of enzyme activity was taken as a measure of refolding. In this assay lactate is converted to pyruvate by LDH with simultaneous reduction of  $\text{NAD}^+$  to NADH which absorbs at 340 nm. The assay mixture contained LDH (0.07  $\mu\text{M}$ ),  $\text{NAD}^+$  (0.2 mM), and sodium lactate (100 mM) in TBS-1 buffer. Reaction was initiated by addition of enzyme, and increase in absorbance at 340 nm due to the reduction of  $\text{NAD}^+$  was monitored at room temperature. The enzyme loses its activity upon denaturation, but activity increases slightly with time if the denatured enzyme is allowed to fold spontaneously as shown in Figure 5.

**Effect of Phosphorylcholine Binding on the Chaperone-like Activity of PDC-109.** Chaperone activity was assayed as described above by monitoring the ability of PDC-109 to prevent heat-induced aggregation of ADH at 48 °C. To probe the effect of ligand binding on the chaperone activity, PDC-109 was incubated for 10 min with different concentrations of PrC before the assay was performed. The reaction mixture contained 60  $\mu\text{g/mL}$  ADH and 40  $\mu\text{g/mL}$  PDC-109 in TBS-1. Aggregation was monitored by recording light scattering at 360 nm in a Cary 100 UV/vis Bio spectrophotometer.

**Effect of Salts on Chaperone-like Activity of PDC-109.** Increase in ionic strength of the medium results in a dissociation of higher aggregates of PDC-109 and yields smaller oligomers (5). Maximal dissociation occurs in high ionic strength buffer containing 50 mM EDTA and 0.5 M NaCl. PDC-109 in 10 mM MOPS buffer (pH 7.4) containing 50 mM EDTA and 0.5 M NaCl was used to check the effect of high ionic strength on the chaperone activity. PDC-109 in the same buffer without salt and EDTA was used as the control. Chaperone activity was studied by ADH aggregation assay as described above.

## RESULTS

PDC-109, the major protein of bovine seminal plasma, appears to be a multifunctional protein as it binds to a variety of molecules including choline phospholipids, apolipoproteins A1 and A2, and heparin (8, 33, 34). However, the precise functional roles played by this protein are not fully clear. Since several characteristics of PDC-109 are akin to the properties exhibited by proteins that act as molecular chaperones such as small heat shock proteins, spectrin, and  $\alpha$ -crystallin, in the present study we investigated whether PDC-109 exhibits chaperone activity. Results from different biophysical studies and biochemical assays indicate that PDC-109 assists in the proper refolding of several other proteins and keeps them active, strongly suggesting that it functions as a molecular chaperone.

**G6PD Activity Assay To Probe Chaperone-like Function of PDC-109.** To investigate whether PDC-109 can prevent the thermal denaturation of G6PD, we assayed the activity of this enzyme in the absence and in the presence of PDC-109. When incubated at 45 °C for 30 min, G6PD lost about 60% of its activity in the absence of PDC-109 (Figure 1A, curve 2), while activity in the presence of PDC-109 was comparable to that of the native enzyme (Figure 1A, curve 3). In control experiments, activity of G6PD alone and G6PD in the presence of PDC-109, incubated at 4 °C, was assayed. Activity of the enzyme solution which was incubated in the presence of PDC-109 at 4 °C was found to be 23% higher than that of the native enzyme (Figure 1A, curve 4). Percent activity of different samples is shown in the form of a bar diagram in Figure 1B.

**Chaperone-like Function of PDC-109 Investigated by Aggregation Assay.** Results of turbidimetric studies aimed at investigating the effect of PDC-109 on the thermal aggregation of ADH are shown in Figure 1C. When ADH was incubated at 48 °C, it is seen that turbidity of the sample increases rapidly with time, reaches a maximum, and then levels off (curve 1). The presence of PDC-109 reduced the rate of this aggregation significantly in a concentration-dependent manner. A PDC-109 to ADH (w/w) ratio of 2:1 led to a considerable reduction in the rate of aggregation (curve 2). The aggregation decreased further when the PDC-109 to ADH ratio was increased to 1:1.4 (curve 3), whereas very little aggregation was observed at a ratio of 1:1 (curve 4). A bar diagram showing percent aggregation versus concentration of PDC-109 is given in Figure 1D. PDC-109 exhibited similar chaperone-like activity on other proteins such as LDH and  $\beta_L$ -crystallin (see Supporting Information Figures S1 and S2).

**PDC-109-Assisted Reactivation of Urea-Denatured GST.** Urea-induced unfolding of GST, which results in a loss of its activity, was monitored by GST-CDNB spectrophotometric assay. It was observed that urea treatment results in a loss of more than 60% of the activity of GST (Figure 1E, curve 2),



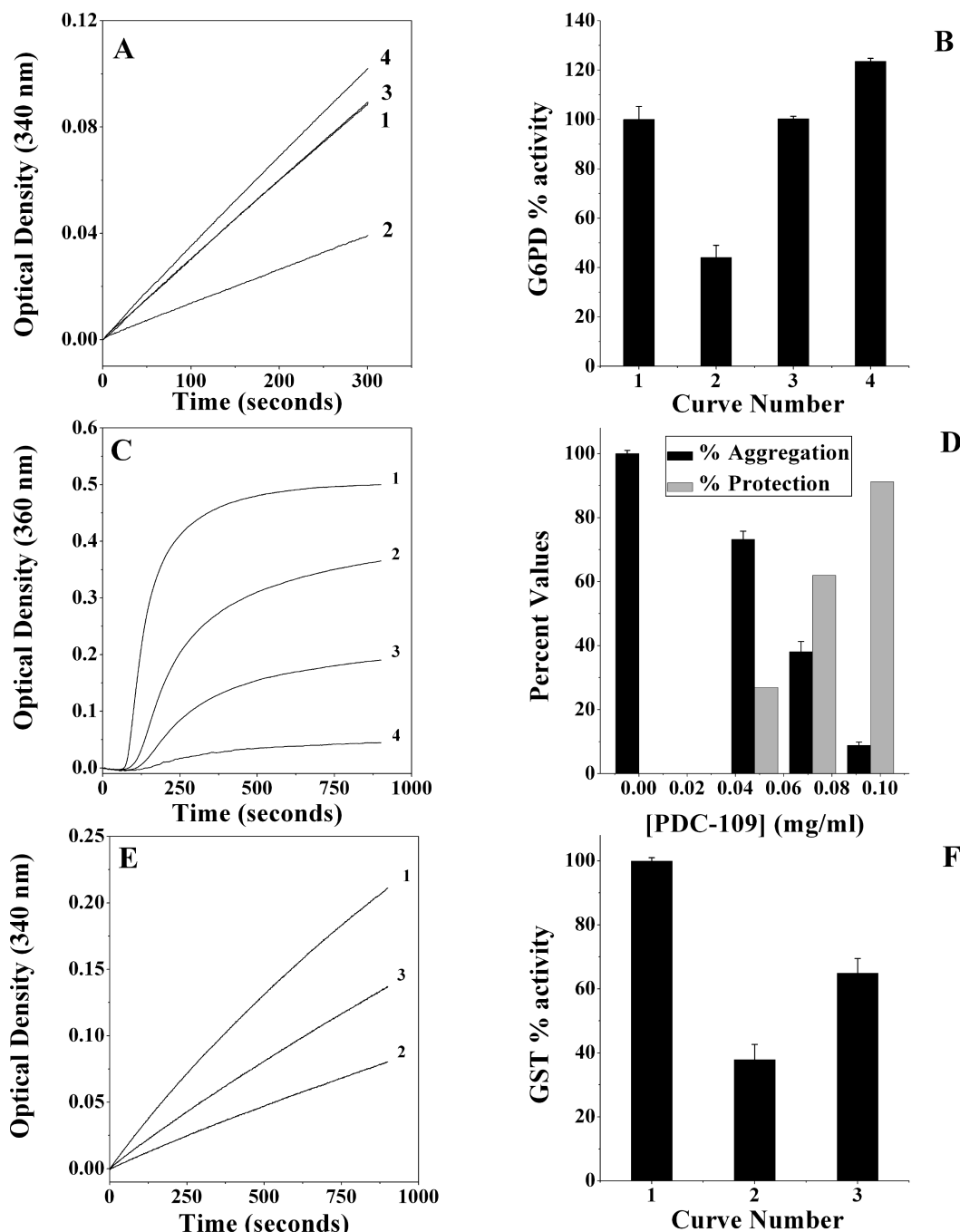


FIGURE 1: PDC-109 exhibits chaperone-like activity against different target proteins. (A) PDC-109-assisted reactivation of G6PD. Activity of the enzyme at room temperature under native conditions (1), after incubation at 45 °C (2), upon incubation at 45 °C in the presence of PDC-109 (3), and after incubation at 4 °C in the presence of PDC-109 (4) is shown. (B) Bar diagram representing the activity of G6PD at 300 s (from panel A). (C) Prevention of aggregation of ADH (0.1 mg/mL) by PDC-109. Aggregation profiles of (1) ADH at 48 °C, (2) ADH + 0.048 mg/mL PDC-109, (3) ADH + 0.072 mg/mL PDC-109, and (4) ADH + 0.096 mg/mL PDC-109 are shown. (D) Bar diagram representing percent aggregation (black bars) and protection (gray bars) of ADH with PDC-109 at different concentrations. (E) Reactivation of urea-denatured GST. Activity of native enzyme at room temperature (1), urea-denatured enzyme (2), and urea-treated GST in the presence of PDC-109 (3). (F) Bar diagram representing the activity of GST at 900 s (from panel E).

whereas in the presence of PDC-109 considerable protection was observed, and its activity was found to be ca. 65% of that observed in its native state (Figure 1E, curve 3). A bar diagram indicating percent activity of different samples with respect to the activity of native GST (taken as 100%) is shown in Figure 1F.

**Prevention of Thermal Aggregation of LDH by PDC-109.** DSC thermograms corresponding to the unfolding of LDH alone and in the presence of different concentrations of PDC-109

are shown in Figure 2. Under native conditions LDH shows an unfolding transition centered at ~54.7 °C, and a steep decline is seen in the baseline above 60 °C. Such steep decrease of the baseline is normally associated with precipitation of the protein, and examination of the sample after completion of the thermal scan confirmed that LDH precipitated during the DSC scan (○). When a mixture of LDH and PDC-109 (1:0.625 w/w) was subjected to DSC analysis, the thermal transition peak of LDH was nearly unaltered, whereas the steeply declining region in the

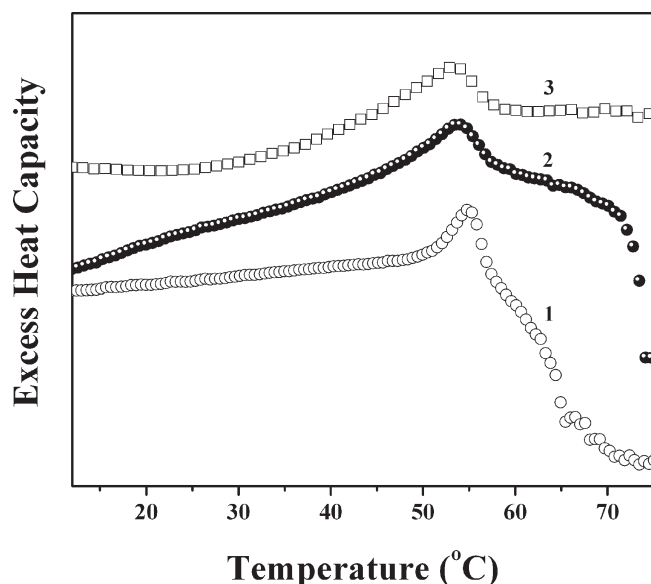


FIGURE 2: Calorimetric studies for PDC-109-induced stabilization of LDH. DSC thermograms shown correspond to 0.4 mg/mL LDH alone (○) and in the presence of 0.25 mg/mL (●) and 0.4 mg/mL (□) PDC-109. See text for details.

thermogram shifted toward higher temperatures ( $> 70^{\circ}\text{C}$ ) (●). However, when the LDH to PDC-109 weight ratio was increased to 1:1, no precipitation of LDH was observed up to  $75^{\circ}\text{C}$  (□).

**PDC-109-Assisted Protection of Insulin under Amyloidogenic Conditions.** Under amyloidogenic conditions (e.g., acidic pH and high temperature) insulin molecules unfold partially and interact with each other to form linear aggregates or fibrils (Figure 3A). However, insulin samples which are subjected to similar conditions in the presence of PDC-109 failed to form such linear aggregates and showed native-like homogeneous distribution (Figure 3B). Inhibition of insulin fibrillation by PDC-109 was also confirmed by fluorometric assay of thioflavin T binding to insulin fibrils (see below).

**Inhibition of Insulin Fibrillation by PDC-109.** Thioflavin T (ThT) is known to bind to amyloid fibrils. Fluorescence emission spectra for the binding of ThT to insulin fibrils in both the absence and presence of PDC-109 are shown in Figure 3. ThT binding to insulin fibrils results in an increase in the intensity of fluorescence maxima of the probe (Figure 3C), whereas in the presence of PDC-109 increase in the fluorescence intensity of ThT was found to be negligible (Figure 3D), which is consistent with the ability of PDC-109 to prevent fibrillation of insulin, as suggested above.

**PDC-109-Mediated Protection of Target Proteins Studied by AFM and Image Analysis.** AFM images of ADH obtained at room temperature indicate that this enzyme shows a uniform distribution and does not form large aggregates (Figure 4A). Upon incubation at  $48^{\circ}\text{C}$  fairly large aggregates of micrometer size are formed (Figure 4B). However, when incubated at the same temperature in the presence of PDC-109, ADH did not form aggregated structures but remained homogeneous similar to the native protein (Figure 4C).

In order to get more quantitative information from the AFM images, average FFT analysis was performed. Average FFT trace values for the native target proteins were observed to be very low. The maximum value obtained for native ADH was 0.75 nm (Figure 4E, curve 1), which increased to 6.6 nm upon heat treatment because of the formation of large clumps (Figure 4E,

curve 2). The presence of PDC-109 significantly reduced the aggregation of ADH, resulting in reduced values of average FFT traces (Figure 4E, curve 3).

Similarly, the distribution density histogram shows a size distribution in the range of 2–7 nm for native ADH (Figure 4F, curve 1). Thermally induced aggregation resulted in an increase in the size distribution to 80–120 nm (Figure 4F, curve 2). The size distribution again shifted toward lower values, viz. 4–10 nm (Figure 4F, curve 3) in the presence of PDC-109, suggesting that this protein prevents the aggregation of the target proteins. Statistical parameters for the native enzyme and enzyme subjected to heat treatment in the absence and presence of PDC-109 are presented in Table 1. Bearing ratio analysis also yielded similar interpretations (see Supporting Information Figure S3). Similar results were obtained with LDH as the target protein (see Supporting Information Figures S4 and S5).

**PDC-109-Assisted Folding Arrest of Target Proteins.** Results of studies aimed at investigating the effect of PDC-109 on the refolding of LDH are shown in Figure 5. Dilution resulted in the spontaneous refolding of completely denatured enzyme, whose activity reaches a maximum level and remains steady afterward (Figure 5A, curve 1). Inclusion of increasing concentrations of PDC-109 in the renaturation buffer resulted in folding arrest, and it was observed to be concentration dependent, i.e., the higher the concentration of PDC-109, the more the arrest (Figure 5A, curves 2–4). Extent of refolding at different concentrations of PDC-109 is shown in the form of bar diagram in Figure 5B. PDC-109 exhibited a similar effect on the refolding of G6PD also (see Supporting Information Figure S6). The presence of ATP did not have any effect on the extent of refolding (data not shown).

**Inhibition of Chaperone Activity of PDC-109 by Phosphorylcholine and Choline.** The effect of PrC binding on the chaperone-like activity of PDC-109 was assessed by turbidimetry, and the results obtained are presented in Figure 6. Incubation of ADH at  $48^{\circ}\text{C}$  resulted in a rapid increase in the turbidity of the solution, which reached a maximum and remained steady thereafter (Figure 6A, curve 1). The presence of PDC-109 resulted in a significant reduction in the aggregation, which was observed to be less than 50% as compared to that of the native enzyme (curve 2). However, addition of increasing concentrations of PrC along with PDC-109 yielded a proportional increase in the extent of aggregation (Figure 6A, curves 3–5). A bar diagram representing percent aggregation of ADH under different conditions is shown in Figure 6B. LDH also showed similar behavior in the presence of PrC (see Supporting Information Figure S7). Choline binding also had a similar effect on the chaperone activity of PDC-109 (see Supporting Information Figure S8).

**Inhibition of Chaperone Activity of PDC-109 in High Ionic Strength Buffer.** Incubation of ADH at  $48^{\circ}\text{C}$  resulted in an increase in the turbidity of the solution, which reached a maximum and then remained constant (Figure 7A, curve 1). However, incubation of ADH with PDC-109 prior to assay resulted in a significant decrease in the turbidity, and it was observed to be less than 20% of the turbidity observed with the sample in the absence of PDC-109 (Figure 7A, curve 2). A bar diagram indicating the relative aggregation of the different samples is given in Figure 7B.

ADH which was incubated at  $48^{\circ}\text{C}$  in high ionic strength buffer (containing 50 mM EDTA and 0.5 M NaCl) yielded a solution that is significantly more turbid as compared to the sample that was incubated in 10 mM buffer without EDTA and

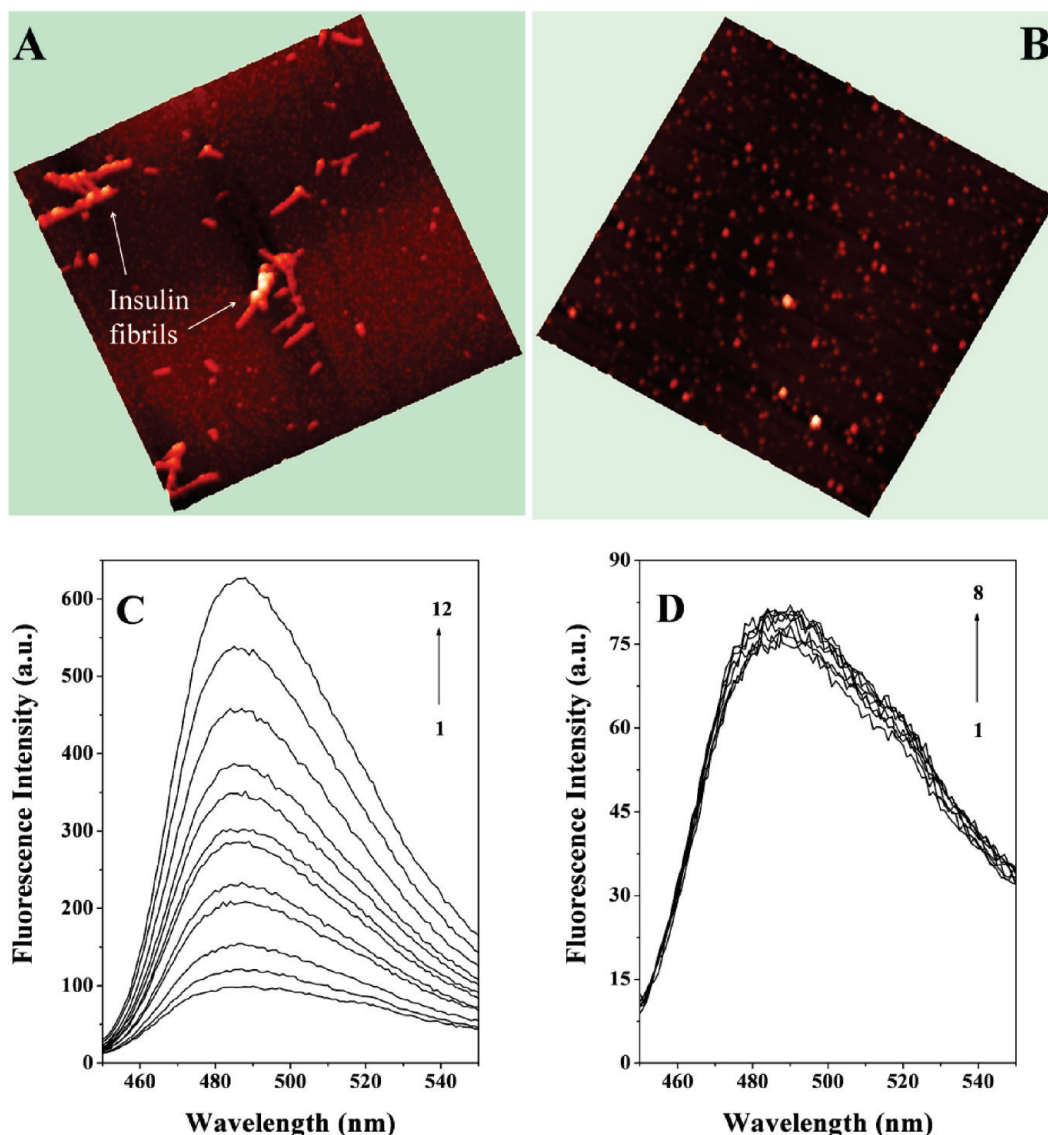


FIGURE 3: Inhibition of insulin fibrillization by PDC-109. (A) AFM image of insulin fibril (0.5 mg/mL, pH 1.6) after incubation at 45 °C for 5 days ( $5 \times 5 \mu\text{m}$  scale). (B) Insulin subjected to similar treatment in the presence of 1.0 mg/mL PDC-109 ( $5 \times 5 \mu\text{m}$  scale). (C) Fluorometric assay for ThT binding to insulin fibrils. Spectrum 1 corresponds to ThT alone (0.1 mM), and spectra 2–12 correspond to those recorded in the presence of increasing concentrations of insulin. The highest insulin concentration was  $6.45 \mu\text{M}$  (spectrum 12). (D) ThT binding to insulin in the presence of PDC-109. Spectrum 1 corresponds to ThT alone (0.1 mM), and spectra 2–8 correspond to those recorded in the presence of increasing concentrations of insulin, which was preincubated with 1.0 mg/mL PDC-109. The highest concentration of insulin was  $4.54 \mu\text{M}$  (spectrum 8).

NaCl (Figure 7C, curve 1). Addition of PDC-109 (in high ionic strength buffer) to ADH did not significantly decrease the aggregation (Figure 7C, curve 2). The relative aggregation of different samples is presented as a bar diagram in Figure 7D.

## DISCUSSION

Molecular chaperones are a diverse class of proteins which play a crucial role in cell physiology under both normal and stressful conditions, by assisting proper folding of newly synthesized proteins as well as misfolded ones. The presence of chaperone proteins in mammalian seminal plasma has not been established so far; however, several somatic and germline-specific molecular chaperones such as calnexin and calnexin have been identified in the male germline (35–38). The present studies demonstrate that the major protein of bovine seminal plasma, PDC-109, can function as a molecular chaperone. To the best of

our knowledge, this is the first study reporting chaperone-like activity of a seminal plasma protein. *In vitro* experiments show functional similarities between PDC-109 and several other well-known chaperone proteins such as  $\alpha$ -crystallin and spectrin.

The results of the present study show that the presence of PDC-109 not only provides protection to target proteins under stress conditions but also directs native proteins to a better conformation even under physiological conditions. Aggregation-prone proteins such as G6PD may also be present in partially aggregated conformations, even under native conditions. PDC-109 appears to interact with such proteins and assist them to a better, functionally active conformation. This is evident from Figure 1A, where the activity of G6PD in the presence of PDC-109 (at 4 °C) was observed to be higher than its activity under native conditions in the absence of PDC-109. CD measurements show that the secondary structure of this protein is largely retained in



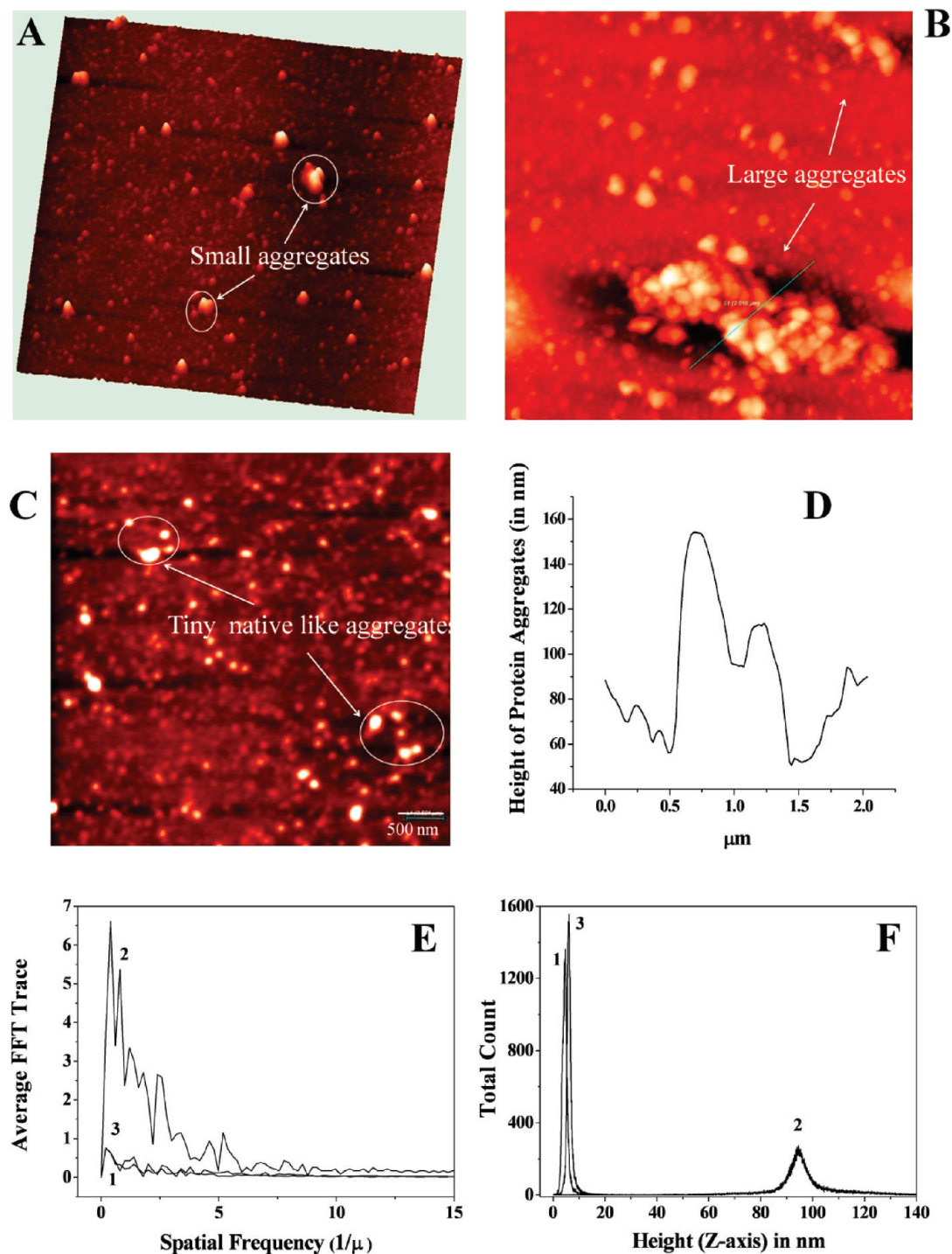


FIGURE 4: Prevention of thermal aggregation of ADH by PDC-109. AFM images of 0.04 mg/mL ADH under native condition (A), upon heat treatment ((B), and upon heat treatment in the presence of 0.02 mg/mL PDC-109 (C) are shown. Each image is  $5 \times 5 \mu\text{m}$  in size. (D) Height profile of aggregated structure (marked in panel B). (E) Average FFT analysis of AFM images of ADH: (1) native enzyme (2) upon incubation at  $48^\circ\text{C}$  and (3) upon incubation at  $48^\circ\text{C}$  in the presence of PDC-109. (F) Distribution density histogram analysis for ADH: (1) native enzyme (2) upon incubation at  $48^\circ\text{C}$  and (3) upon incubation at  $48^\circ\text{C}$  in the presence of PDC-109. See text for details.

Table 1: Parameters Obtained from Statistical Analysis of AFM Images of Alcohol Dehydrogenase under Different Experimental Conditions

sample	amount of sampling (pixels)	max height (nm)	mean height (nm)	entropy
native enzyme	65536	20.6	4.68	6.66
enzyme at $48^\circ\text{C}$	65536	163.00	96.5	9.86
enzyme + PDC-109 at $48^\circ\text{C}$	65536	33.2	6.4	6.62

the presence of PDC-109 even at elevated temperatures, whereas in the absence of PDC-109 the secondary structure

is altered significantly (Supporting Information Figure S9). This shows that PDC-109 is able to protect G6PD from



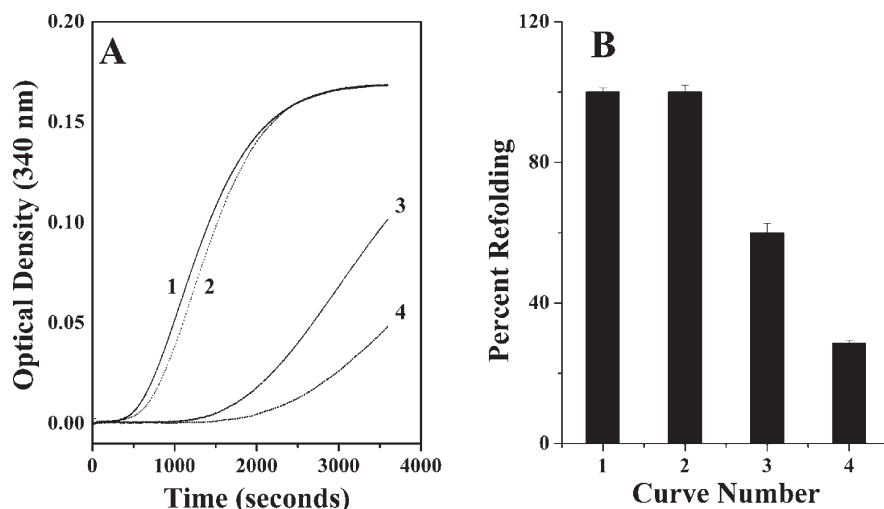


FIGURE 5: Refolding of LDH in the absence and presence of PDC-109. (A) LDH was refolded from the completely unfolded state in the absence (curve 1) as well as presence of different concentrations of PDC-109 in TBS-I buffer as indicated: 0.35  $\mu$ M (curve 2), 3.5  $\mu$ M (curve 3), and 5.36  $\mu$ M (curve 4). (B) Bar diagram showing the extent of refolding under different conditions.

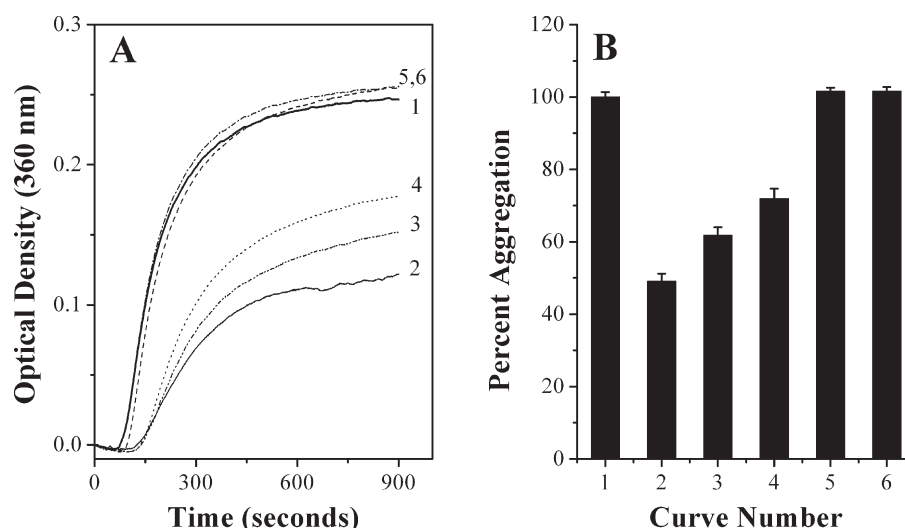


FIGURE 6: Effect of phosphorylcholine binding on the chaperone-like activity of PDC-109. (A) Aggregation profiles of ADH incubated at 48 °C in the absence and presence of PDC-109 and phosphorylcholine. The samples are (1) ADH at 48 °C, (2) ADH + PDC-109, (3) ADH + PDC-109 + 0.01 mM PrC, (4) ADH + PDC-109 + 0.05 mM PrC, (5) ADH + PDC-109 + 0.1 mM PrC, and (6) ADH + 0.05 mM PrC. Concentrations of ADH and PDC-109 were 0.06 and 0.04 mg/mL, respectively. (B) Bar diagram representing the aggregation of ADH in the different samples.

thermal unfolding and provides an explanation for the retention of its activity at elevated temperatures in the presence of PDC-109. Natively unfolded proteins such as  $\alpha$ -synuclein have been reported to be good candidates for chaperone-like activity because of the flexibility of their structure, which allows them to interact with other proteins in an effective manner (39). PDC-109 also possesses a significant amount of unordered structure (5, 6), which is consistent with its ability to function as a molecular chaperone.

Results of turbidimetric studies to monitor thermally induced aggregation of ADH and LDH suggest that PDC-109 functions as a chaperone in a concentration-dependent manner; i.e., the chaperone activity increases with increasing concentrations of PDC-109 (Figure 1C and Supporting Information Figure S1). Since isozymes of LDH such as LDH-C<sub>4</sub> participate in mammalian sperm capacitation process (40, 41), the chaperone-like activity of PDC-109 observed with LDH *in vitro* may be relevant to a similar function under *in vivo* conditions.

AFM experiments provide further strong evidence for the chaperone-like activity of PDC-109. To the best of our knowledge, this is the first time that the potential of image processing of AFM data, demonstrating clear-cut differences between aggregated and disaggregated proteins, has been utilized to probe the chaperone-like activity of any protein. Both ADH and LDH upon exposure to high temperature form large aggregates as can be judged by larger values of average FFT and were distributed mostly in low frequency domains, which means they were spaced apart and hence were distributed inhomogeneously (Figure 4E, curve 2; Supporting Information Figure S5A, curve 2). However, protein molecules subjected to similar treatment in the presence of PDC-109 were found to be distributed almost equally in all frequency domains, similar to the native protein molecules (Figure 4E, curves 1 and 3; Supporting Information Figure S5A, curves 1 and 3). Uniform distribution of target protein molecules which have been subjected to heat treatment in the presence of PDC-109 is also evident from the lesser entropy values observed for such samples, whereas higher entropy values

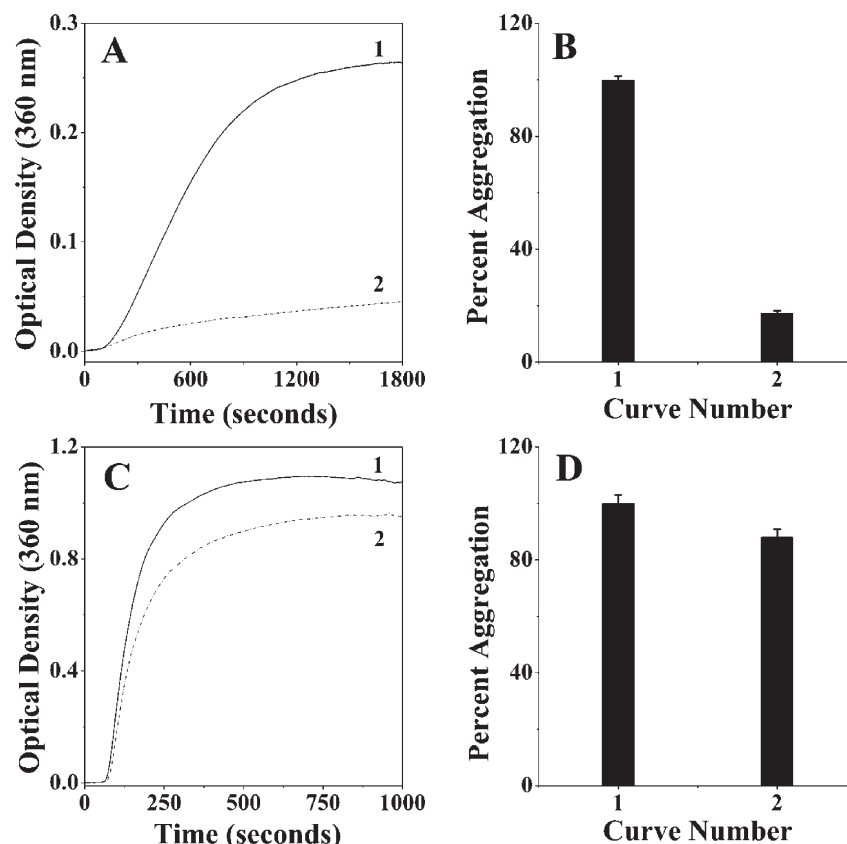


FIGURE 7: Effect of high ionic strength on chaperone-like activity of PDC-109. (A) Aggregation profile of native ADH at 48 °C in 10 mM MOPS buffer in the absence (curve 1) and presence of 0.027 mg/mL PDC-109 (curve 2). (B) Bar diagram representing the level of aggregation in 10 mM MOPS buffer. (C) Aggregation profile of native ADH at 48 °C in 10 mM high ionic strength MOPS buffer (containing 50 mM EDTA and 0.5 M NaCl) in the absence (curve 1) and presence of 0.027 mg/mL PDC-109 (curve 2). (D) Bar diagram representing the level of aggregation in 10 mM high ionic strength MOPS buffer. ADH concentration was 0.2 mg/mL for all of the experiments.

obtained with aggregated proteins suggest their random distribution (Table 1). The present study also explores the potential of PDC-109 to prevent the fibrillation of amyloid-prone proteins such as insulin. This can be of promising significance because some of the proteins of the seminal plasma have been identified to be prone to amyloidogenesis (42, 43).

Experiments aimed at investigating the effect of PDC-109 on the refolding of fully denatured target proteins suggest that PDC-109 binds to unfolded substrate proteins and forms stable complexes with them. This prevents their irreversible aggregation but does not assist their refolding to the native form; i.e., PDC-109 binding results in a *folding arrest* of the target proteins (Figure 5). In this respect, PDC-109 is similar to spectrin and Hsp90 (27, 28). However, unlike these two chaperone proteins, PDC-109 does not assist the refolding of target proteins in the presence of ATP. Although this folding arrest of substrate proteins by PDC-109 suggests that it creates a reservoir of folding intermediates of the substrate proteins (44, 45), it should be noted that unlike other such proteins (e.g., murine Hsp25 and yeast Hsp26), which cannot prevent inactivation of the substrate proteins, under stress conditions the activity of target proteins in the presence PDC-109 was found to be comparable to that of the native form (Figure 1A).

Binding of phosphorylcholine or choline to PDC-109 resulted in a complete inhibition of its chaperone-like activity in a concentration-dependent manner (Figure 6, Supporting Information Figures S7 and S8). Since the specific binding of these ligands to the FnII domains of PDC-109 leads to dissociation of the polydisperse aggregates of the protein, resulting in the

formation of dimeric species (5), it is likely that the ligand binding site or the aggregation state of the protein is important for the chaperone activity of PDC-109. In order to understand this better, we investigated the effect of high ionic strength in the medium, which is known to result in a dissociation of the polydisperse aggregates of PDC-109 to yield smaller oligomers (5), on the chaperone-like activity of the protein. These experiments indicated that the chaperone-like activity of PDC-109 is reduced significantly in high ionic strength medium (Figure 7), suggesting that the state of aggregation is an important factor which modulates the chaperone-like activity of this protein.

Pairwise sequence alignment studies show significant sequence homology and analogy between PDC-109 and other well-known chaperone-like proteins (Supporting Information Table S1 and Figure S10). These observations are consistent with the present findings, which demonstrate that PDC-109 exhibits chaperone-like activity against a range of target proteins.

On the basis of experimental evidence presented above, we propose a possible mechanism for the involvement of PDC-109 in the sperm capacitation process. It has been demonstrated by Manjunath and co-workers that PDC-109 induces the efflux of cholesterol and choline phospholipids from sperm membrane, which facilitates sperm capacitation (8, 16, 17). Here we suggest an additional function for this protein, where PDC-109 may direct the aggregated and misfolded proteins of seminal plasma, sperm plasma membrane, or other proteins of surrounding environment toward a functionally active, folded conformation, which can then participate in the fertilization process in a better way. A schematic representation of this hypothesis is shown in

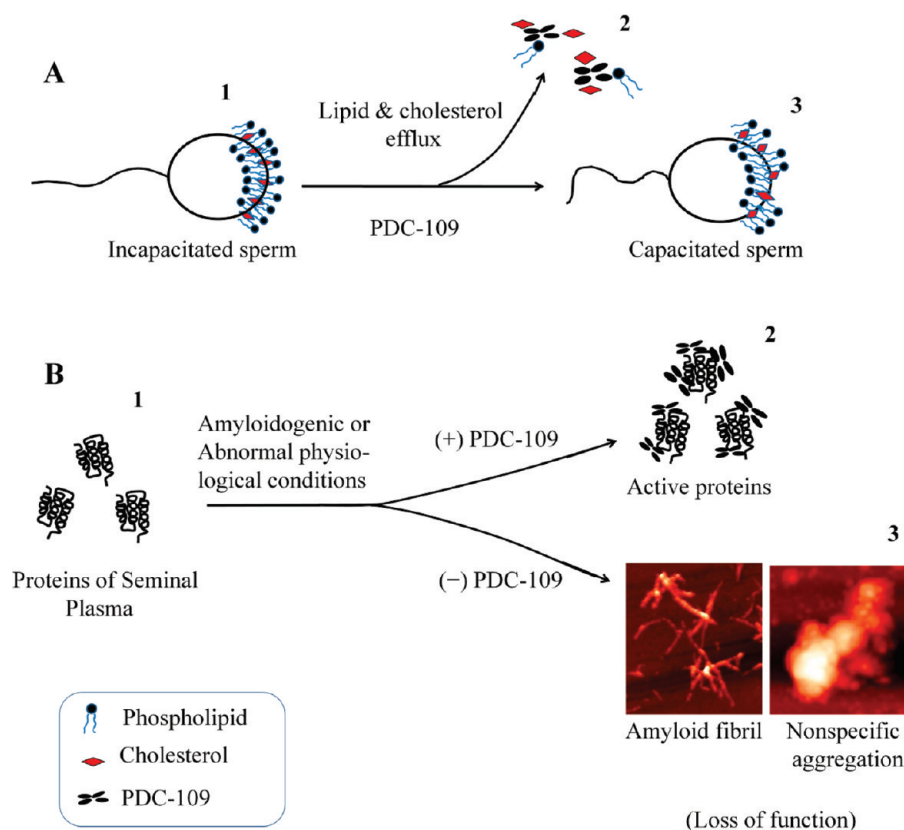


FIGURE 8: A schematic model for PDC-109-induced sperm capacitation. (A) PDC-109 induces efflux of cholesterol and choline phospholipids, which is necessary for sperm capacitation. Epididymal spermatozoa (1), efflux particles made up of PDC-109, cholesterol, and choline phospholipids (2), and capacitated sperm (3) are shown. (B) PDC-109 functions as a molecular chaperone and stabilizes seminal plasma proteins. Seminal plasma proteins (1) are stabilized in the presence of PDC-109 under stress conditions (2), which in the absence of PDC-109 may form nonspecific aggregates or amyloid fibrils (3).

Figure 8. A search for seminal plasma proteins that are homologous to PDC-109 showed moderate to high homology with proteins from different species such as horse, pig, and human (Supporting Information Figure S11 and Table S2) and indicates that these proteins may also exhibit chaperone-like activity.

## CONCLUSION

In summary, in this study several lines of evidence are presented to show that the major protein of bovine seminal plasma, PDC-109, exhibits chaperone-like activity, which may be relevant to sperm capacitation. Biochemical assays and biophysical methods have shown that PDC-109 effectively protects a variety of target proteins from denaturation induced by heat, chaotropes, and low pH. AFM studies have shown that PDC-109 prevents fibrillation of insulin under amyloidogenic conditions, which is of considerable significance since amyloidogenesis is a serious problem during sperm maturation in certain species. Overall, these results demonstrate that PDC-109 functions as a molecular chaperone, suggesting that it may assist the proper folding of proteins in bovine seminal plasma *in vivo*.

## ACKNOWLEDGMENT

We are grateful to Dr. K. Babu Rao of the Lam Farm, Guntur, Sri Venkateswara Veterinary University, for kindly providing samples of bovine semen.

## SUPPORTING INFORMATION AVAILABLE

Additional information relevant to this report containing methodology used in sequence alignments and AFM data

analysis as well as Tables S1 and S2 and Figures S1–S11. This material is available free of charge via the Internet at <http://pubs.acs.org>.

## REFERENCES

- Shivaji, S., Scheit, K. H., and Bhargava, P. M. (1990) Proteins of seminal plasma, pp 1–526, Wiley, New York.
- Esch, F. S., Ling, N. C., Bohlen, P., Ying, S. Y., and Guillemin, R. (1983) Primary structure of PDC-109, a major protein constituent of bovine seminal plasma. *Biochem. Biophys. Res. Commun.* 113, 861–867.
- Baker, M. E. (1985) The PDC-109 protein from bovine seminal plasma is similar to the gelatin-binding domain of bovine fibronectin and a kringle domain of human tissue-type plasminogen activator. *Biochem. Biophys. Res. Commun.* 130, 1010–1014.
- Swamy, M. J. (2004) Interaction of bovine seminal plasma proteins with model membranes and sperm plasma membranes. *Curr. Sci.* 87, 203–211.
- Gasset, M., Saiz, J. L., Sanz, L., Gentzel, M., Töpfer-Petersen, E., and Calvete, J. J. (1997) Conformational features and thermal stability of bovine seminal plasma protein PDC-109 oligomers and phosphorylcholine-bound complexes. *Eur. J. Biochem.* 250, 735–744.
- Wah, D. A., Fernández-Tornero, C., Sanz, L., Romero, A., and Calvete, J. J. (2002) Sperm coating mechanism from the 1.8 Å crystal structure of PDC-109-phosphorylcholine complex. *Structure* 10, 505–514.
- Calvete, J. J., Raida, M., Sanz, L., Wempe, F., Scheit, K. H., Romer, A., and Töpfer-Petersen, E. (1994) Localization and structural characterization of an oligosaccharide O-linked to bovine PDC-109. Quantitation of the glycoprotein in seminal plasma and on the surface of ejaculated and capacitated spermatozoa. *FEBS Lett.* 350, 203–206.
- Desnoyers, L., and Manjunath, P. (1992) Major proteins of bovine seminal plasma exhibit novel interactions with phospholipids. *J. Biol. Chem.* 267, 10149–10155.
- Ramakrishnan, M., Anbazhagan, V., Pratap, T. V., Marsh, D., and Swamy, M. J. (2001) Membrane insertion and lipid-protein interactions of bovine seminal plasma protein, PDC-109 investigated by spin label electron spin resonance spectroscopy. *Biophys. J.* 81, 2215–2225.

10. Greube, A., Müller, K., Töpfer-Petersen, E., Herrmann, A., and Müller, P. (2001) Influence of the bovine seminal plasma protein PDC-109 on the physical state of membrane. *Biochemistry* 40, 8326–8334.
11. Thomas, C. J., Anbazhagan, V., Ramakrishnan, M., Sultan, N., Surolia, I., and Swamy, M. J. (2003) Mechanism of membrane binding by the bovine seminal plasma protein, pdc-109, a surface plasmon resonance study. *Biophys. J.* 84, 3037–3044.
12. Swamy, M. J., Marsh, D., Anbazhagan, V., and Ramakrishnan, M. (2002) Effect of cholesterol on the interaction of seminal plasma protein, PDC-109 with phosphatidylcholine membranes. *FEBS Lett.* 528, 230–234.
13. Anbazhagan, V., and Swamy, M. J. (2005) Thermodynamics of phosphorylcholine and lysophosphatidylcholine binding to the major protein of bovine seminal plasma, PDC-109. *FEBS Lett.* 579, 2933–2938.
14. Anbazhagan, V., Damai, R. S., Paul, A., and Swamy, M. J. (2008) Interaction of the major protein from bovine seminal plasma, pdc-109 with phospholipid membranes and soluble ligands investigated by fluorescence approaches. *Biochim. Biophys. Acta* 1784, 891–899.
15. Damai, R. S., Anbazhagan, V., Rao, K. B., and Swamy, M. J. (2009) Fluorescence studies on the interaction of choline-binding domain b of the major bovine seminal plasma protein, pdc-109 with phospholipid membranes. *Biochim. Biophys. Acta* 1794, 1725–1733.
16. Thérien, I., Moreau, R., and Manjunath, P. (1998) Major proteins of bovine seminal plasma and high-density lipoprotein induce cholesterol efflux from epididymal sperm. *Biol. Reprod.* 59, 768–776.
17. Moreau, R., Thérien, I., Lazure, C., and Manjunath, P. (1998) Type II domains of BSP-A1/A2 proteins: binding properties, lipid efflux and sperm capacitation potential. *Biochem. Biophys. Res. Commun.* 246, 148–154.
18. Lindquist, S., and Craig, E. A. (1988) The heat-shock proteins. *Annu. Rev. Genet.* 22, 631–677.
19. Horwitz, J. (1992) Alpha-crystallin can function as a molecular chaperone. *Proc. Natl. Acad. Sci. U.S.A.* 89, 10449–10453.
20. Datta, S. A., and Rao, C. M. (1999) Differential temperature-dependent chaperone-like activity of  $\alpha$ A- and  $\alpha$ B-crystallin homo-aggregates. *J. Biol. Chem.* 274, 34773–34778.
21. Reddy, G. B., Das, K. P., Petrash, J. M., and Surewicz, W. K. (2000) Temperature-dependent chaperone activity and structural properties of human  $\alpha$ A- and  $\alpha$ B-crystallins. *J. Biol. Chem.* 275, 4565–4570.
22. Das, K. P., and Surewicz, W. K. (1995) On the substrate specificity of  $\alpha$ -crystallin as a molecular chaperone. *Biochem. J.* 311, 367–370.
23. Qu, J., Susanne, B.-K., Holst, O., and Kleinschmidt, J. H. (2009) Binding regions of outer membrane protein A in complexes with the periplasmic chaperone Skp. A site-directed fluorescence study. *Biochemistry* 48, 4926–4936.
24. Rao, P. V., Huang, Q. L., Horwitz, J., and Zigler, J. S., Jr. (1995) Evidence that alpha-crystallin prevents non-specific protein aggregation in the intact eye lens. *Biochim. Biophys. Acta* 1245, 439–447.
25. Wang, K., and Spector, A. (1994) The chaperone activity of bovine  $\alpha$ -crystallin. *J. Biol. Chem.* 269, 13601–13608.
26. Rajaraman, K., Raman, B., and Rao, C. M. (1996) Molten-globule state of carbonic anhydrase binds to the chaperone-like alpha-crystallin. *J. Biol. Chem.* 271, 27595–27600.
27. Chakrabarti, A., Bhattacharya, S., Ray, S., and Bhattacharya, M. (2001) Binding of a denatured heme protein and ATP to erythroid spectrin. *Biochem. Biophys. Res. Commun.* 282, 1189–1193.
28. Yonehara, M., Minami, Y., Kawata, Y., Nagai, J., and Yahara, I. (1996) Heat-induced chaperone activity of Hsp90. *J. Biol. Chem.* 271, 2641–2645.
29. Kumar, M. S., Reddy, P. Y., Sreedhar, B., and Reddy, G. B. (2005)  $\alpha$ B-Crystallin assisted reactivation of glucose-6-phosphate dehydrogenase upon refolding. *Biochem. J.* 391, 335–341.
30. Habig, W. H., Pabst, M. J., and Jakoby, W. B. (1974) Glutathione-S-transferase: the first enzymatic step in mercapturic acid formation. *J. Biol. Chem.* 249, 7130–7139.
31. Wang, H., Duennwald, M. L., Roberts, B. E., Rozeboom, L. M., Zhang, Y. L., Steele, A. D., Krishnan, R., Su, L. J., Griffin, D., Mukhopadhyay, S., Hennessy, E. J., Weigele, P., Blanchard, B. J., King, J., Deniz, A. A., Buchwald, S. L., Ingram, V. M., Lindquist, S., and Shorter, J. (2008) Direct and selective elimination of specific prions and amyloids by 4,5-dianilinophthalimide and analogs. *Proc. Natl. Acad. Sci. U.S.A.* 105, 7159–7164.
32. El Feninat, F., Elouatik, S., Ellis, T. H., Sacher, E., and Stangel, I. (2001) Quantitative assessment of surface roughness as measured by AFM: application to polished human dentin. *Appl. Surf. Sci.* 183, 205–215.
33. Manjunath, P., Nauc, V., Bergeron, A., and Menard, M. (2002) Major proteins of bovine seminal plasma bind to the low density lipoprotein fraction of hen's egg yolk. *Biol. Reprod.* 67, 1250–1258.
34. Chandonnet, L., Roberts, K. D., Chapdelaine, A., and Manjunath, P. (1990) Identification of heparin-binding proteins in bovine seminal plasma. *Mol. Reprod. Dev.* 26, 313–318.
35. Ikawa, M., Wada, I., Kominami, K., Watanabe, D., Toshimori, K., Nishimune, Y., and Okabe, M. (1997) The putative chaperone calnexin is required for sperm fertility. *Nature* 387, 607–611.
36. Bergeron, J. J., Brenner, M. B., Thomas, D. Y., and Williams, D. B. (1994) Calnexin: a membrane-bound chaperone of the endoplasmic reticulum. *Trends Biochem. Sci.* 19, 124–128.
37. Miller, D., Brough, S., and al-Harbi, O. (1992) Characterization and cellular distribution of human spermatozoal heat shock proteins. *Hum. Reprod.* 7, 637–645.
38. Mitchell, L. A., Nixon, B., and Aitken, R. J. (2007) Analysis of chaperone proteins associated with human spermatozoa during capacitation. *Mol. Hum. Reprod.* 13, 605–613.
39. Kim, T. D., Paik, S. R., Yang, C. H., and Kim, J. (2000) Structural changes in  $\alpha$ -synuclein affect its chaperone like activity in vitro. *Protein Sci.* 9, 2489–2496.
40. O'Flaherty, C. M., Beorlegui, N. B., and Beconi, M. T. (2002) Lactate dehydrogenase-C4 is involved in heparin and NADH-dependent sperm capacitation. *Andrologia* 34, 91–97.
41. Duan, C., and Goldberg, E. (2003) Inhibition of lactate dehydrogenase C4 (LDH-C4) blocks capacitation of mouse sperm in vitro. *Cytogenet. Genome Res.* 103, 352–359.
42. Münch, J., Rücker, E., Ständker, L., Adermann, K., Goffinet, C., Schindler, M., Wildum, S., Chinnadurai, R., Rajan, D., Specht, A., Giménez-Gallego, G., Sánchez, P. C., Flower, D. M., Koulov, A., Kelly, J. W., Mothes, W., Grivel, J.-C., Margolis, L., Keppler, O. T., Forssmann, W.-G., and Kirchhoff, F. (2007) Semen-derived amyloid fibrils drastically enhance HIV infection. *Cell* 131, 1059–1071.
43. Pitkänen, P., Westermark, P., Cornwell, G. G., III, and Murdoch, W. (1983) Amyloid of the seminal vesicles. A distinctive and common localized form of senile amyloidosis. *Am. J. Pathol.* 110, 64–69.
44. Ehrnsperger, M., Gräber, S., Gaestel, M., and Buchner, J. (1997) Binding of non-native protein to Hsp25 during heat shock creates a reservoir of folding intermediates for refolding. *EMBO J.* 16, 221–229.
45. Nakamoto, H., and Vigh, L. (2007) The small heat shock proteins and their clients. *Cell. Mol. Life Sci.* 64, 294–306.